Toxicology Mechanisms and Methods

http://informahealthcare.com/txm
ISSN: 1537-6516 (print), 1537-6524 (electronic)

Toxicol Mech Methods, 2014; 24(7): 470–487
 DOI: 10.3109/15376516.2014.943441

informa healthcare

RESEARCH ARTICLE

In vitro systems toxicology approach to investigate the effects of repeated cigarette smoke exposure on human buccal and gingival organotypic epithelial tissue cultures

Walter K. Schlage*, Anita R. Iskandar*, Radina Kostadinova*, Yang Xiang*, Alain Sewer*, Shoaib Majeed, Diana Kuehn, Stefan Frentzel, Marja Talikka, Marcel Geertz, Carole Mathis, Nikolai Ivanov, Julia Hoeng, and Manuel C. Peitsch

Philip Morris International R&D, Philip Morris Products S.A., Neuchâtel, Switzerland

Abstract

Smoking has been associated with diseases of the lung, pulmonary airways and oral cavity. Cytologic, genomic and transcriptomic changes in oral mucosa correlate with oral pre-neoplasia, cancer and inflammation (e.g. periodontitis). Alteration of smoking-related gene expression changes in oral epithelial cells is similar to that in bronchial and nasal epithelial cells. Using a systems toxicology approach, we have previously assessed the impact of cigarette smoke (CS) seen as perturbations of biological processes in human nasal and bronchial organotypic epithelial culture models. Here, we report our further assessment using *in vitro* human oral organotypic epithelium models. We exposed the buccal and gingival organotypic epithelial tissue cultures to CS at the air–liquid interface. CS exposure was associated with increased secretion of inflammatory mediators, induction of cytochrome P450s activity and overall weak toxicity in both tissues. Using microarray technology, gene-set analysis and a novel computational modeling approach leveraging causal biological network models, we identified CS impact on xenobiotic metabolism-related pathways accompanied by a more subtle alteration in inflammatory processes. Gene-set analysis further indicated that the CS-induced pathways in the *in vitro* buccal tissue models resembled those in the *in vivo* buccal biopsies of smokers from a published dataset. These findings support the translatability of systems responses from *in vitro* to *in vivo* and demonstrate the applicability of oral organotypical tissue models for an impact assessment of CS on various tissues exposed during smoking, as well as for impact assessment of reduced-risk products.

Keywords

Air–liquid interface, causal biological network model, oral keratinocytes, organotypic cultures, transcriptomics

History

Received 15 April 2014
Revised 20 June 2014
Accepted 29 June 2014
Published online 11 September 2014

Introduction

Cigarette smoke (CS)-related morbidity and mortality are often linked to lung cancer and chronic obstructive pulmonary disease. However, CS is also associated with cancer and inflammatory diseases of the oral cavity (Office of the Surgeon General US, 2004; Sasco et al, 2004; Warnakulasuriya et al., 2010; Winn, 2001). In addition, cytologic, genomic and transcriptomic changes in oral mucosa correlate not only with oral inflammatory diseases (e.g. periodontitis), but also with pre-neoplasia and cancers of the aero-digestive tract (Banerjee et al., 2005; Khan et al., 2011; Noutomi et al., 2006; Proia et al., 2006; Toruner et al., 2004; Watanabe et al., 2009; Zhang & Rosin, 2001).

More recent studies, which benefited from high-throughput technologies, have indicated that the changes of gene expression induced by CS in the upper respiratory tract (e.g. nasal and oral tissues) were similar to those in the lower respiratory tract (e.g. bronchial tissue). These observations suggest a common effect of CS in epithelial cells exposed during smoking, including those lining the mouth, nose and bronchus (Sridhar et al., 2008). The ''field of injury'' hypothesis has been proposed to explain these similar CS-related changes in the gene expression that occur throughout the respiratory tract of patients with lung cancer (Gower et al., 2011; Spira et al., 2007; Sridhar et al., 2008; Steiling et al., 2008). Correlations between the gene expression changes in these tissues could be leveraged for the development of biomarkers of CS-exposure or CS-associated lung diseases, particularly using the more accessible tissues, such as nasal or oral tissues, in which detectable histological and/or phenotypical changes are frequently absent (Gower et al., 2011; Spira et al., 2007; Sridhar et al., 2008; Steiling et al., 2008). Due to the relatively non-invasive sampling procedures, this

*These authors are equally contributed to this study.

Address for correspondence: Anita R. Iskandar, Philip Morris International R&D, Philip Morris Products S.A., Quai Jeanrenaud 5, 2000 Neuchâtel, Switzerland. Tel: +41 58 242 2777. E-mail: Anita.Iskandar@pmi.com

approach could be practically implemented in large epidemiological studies (Boyle et al., 2010; Kupfer et al., 2010; Paszkiewicz et al., 2008; Spivack et al., 2004).

Recently, organotypic 3D *in vitro* culture models of the airway epithelia have been used for the assessment of aerosol exposure, e.g. airborne toxicants, environmental toxicants or consumer products (Aufderheide et al., 2011; Combes, 2004). They permit extensive exposure under controlled conditions as needed, such as for mechanistic investigations, environmental studies and product testing (Aufderheide et al., 2011; Combes, 2004). For inhalation studies, the organotypic tissue culture models better reflect the *in vivo* exposure situation because they can be directly exposed to whole CS (aerosol) at the air–liquid interface. In addition, organotypic culture models can potentially be cultured for a longer-term, thus making them useful for assessing the effects of exposure (of conventional CS or reduced-risk products) over extended periods of time (Chinnathambi et al., 2003) and potentially for assessing the effects of smoking cessation. Until today, many aerosol exposure studies have primarily been conducted using bronchial organotypic epithelial models (Balharry et al., 2008; Mathis et al., 2013; Maunders et al., 2007). However, the utilization of oral organotypic tissue models (e.g. buccal or gingival) is seldom despite researchers have shown that the reconstituted organotypic tissues of the oral cavity, e.g. 3D oral mucosal tissues, express differentiated characteristics comparable to the *in vivo* situation and can be used to study innate immunity and pathobiology of the oral mucosa, including gingivitis, candidiasis, oral cancer and inflammation (Andrian et al., 2004; Ceder et al., 2007; Hansson et al., 2001; Klausner et al., 2007; Mostefaoui et al., 2002; Moyes et al., 2010; Walle et al., 2006; Wang e al., 2001). To our knowledge, this study would be the first to report the effects of CS exposure on oral organotypic tissue models at their air–liquid interface. We utilized the 3D reconstructs of human oral buccal epithelium (EpiOral™, MatTek) and gingival epithelium (EpiGingival™, MatTek) that exhibit *in vivo*-like morphological and growth characteristics. Both tissue models are cultured on permeable porous membranes. The tissue models form a multilayered mucosal tissue consisting of a fibroblast-containing lamina propria compartment that is covered by stratified keratinized epithelium (i.e. EpiGingival™) or non-keratinized epithelium (i.e. EpiOral™, which also contains Langerhans cells). These 3D tissue models can be grown to form a full-thickness mucosa consisting of 20–30 layers of epithelial cells and submucosal lamina propria layers including inflammatory cells to recreate the inflammatory responses.

In this study, the impact of CS with its complex nature on these oral tissue models was assessed not only using classical endpoints of cellular response and toxicity assays – i.e. lactate dehydrogenase (LDH) release assay, transepithelial electrical resistance (TEER) assay, histology analysis, Luminex-based measurement of inflammatory markers and cytochrome P450s (CYP) activity measurement – but also using transcriptomics, gene-set analysis and a network-based systems biology approach. The overall objective was to comprehensively investigate the biological impact of CS exposure. One of our approaches included the utilization of the recently published collection of hierarchically structured biological network models to capture biological processes and mechanisms that are specific and relevant to the respiratory system: Cell Proliferation network (Westra et al., 2011), Cell Stress (referred to as Stress) network (Schlage et al., 2011), DNA Damage, Autophagy, Cell Death and Senescence network (Gebel et al., 2013) and the Pulmonary Inflammation Processes network (Westra et al., 2013). These biological network models were built based on *a priori* knowledge of cause-and-effect relationships among biological entities derived from published literature within a specific boundary, i.e. mainly within the context of non-diseased mammalian pulmonary tissues and cardiovascular tissues (Thomson et al., 2013). Because the hierarchical network models are capturing mechanisms at the levels of biological processes, pathways and specific molecular entities; the network models would be useful to not only assess the overall impact of exposure but also to investigate the specific molecular mechanisms affected by the exposure. Using the network models and systems biology approaches, we assessed the impacts of CS exposure (perturbation of the biological networks) that were quantitatively computed from transcriptomics data generated from the tissue models (exposed and non-exposed) as described previously (Hoeng et al., 2012; Thomson et al., 2013).

Altogether, this study aims to examine the overall response of buccal and gingival organotypic tissue cultures to repeated exposure of CS by using a combination of classical cytotoxicity assays and systems toxicology approaches. We use 3D buccal and gingival tissue models (EpiOral™ and EpiGingival™) containing fibroblast layers in both tissues to study the effects and molecular mechanisms of repeated CS exposure. Using the systems biology approach, our results indicated that the repeated CS exposure affected xenobiotic metabolism and inflammatory responses in the tissue models. A weak overall toxicity impact of CS was detected by classical toxicological methods. Furthermore, the results suggest that the effects of CS exposure to the buccal tissues were aligned with those in the buccal samples of smokers, supporting the applicability of oral tissue models for translational research.

Materials and methods

Organotypic tissue culture models

EpiOral™ (buccal) full-thickness epithelial tissues co-cultured with both fibroblasts and Langerhans cells (ORL-300-FT-LC, lot 17943) and EpiGingival™ full-thickness epithelial tissues co-cultured with fibroblasts (GIN-300-FT-1, lot 17942) were purchased from MatTek (Ashland, MA). The buccal and gingival epithelial cells were all isolated from the same donor, a non-smoking 46-year-old man. The fibroblasts (used in both tissues) were isolated from the gingival tissue of the same donor. Both tissue models were cultured at the air–liquid interface in 0.7 ml media in separate 24-well plates [Transwell inserts of 6.5 mm in diameter on a polycarbonate membrane with a pore size of 0.4 μm (Corning product cat #3413)]. Upon delivery, the buccal and gingival tissues were 14 d old. The organotypic models were maintained in house at 37 °C for 3–4 d (before the exposure experiment) at the air–liquid interface with fresh media (GIN-300-FT-MM for the gingival tissue and ORAL-300-FT-MM for the buccal tissue) changed every 2 d according to the supplier's instructions

(MatTek). Following the exposure, the tissues were kept in 2–2.5 ml medium in 6-well plates for up to 48 h. The integrity of the tissue inserts was monitored by: (i) microscopic examination, (ii) the absence of medium leakage and (iii) measurement of TEER. The allocation of the tissue cultures to various endpoints ($N = 3$ inserts following a single exposure run) is depicted in Supplemental Table S1.

VITROCELL® cigarette whole smoke exposure

The reference cigarettes 3R4F were obtained from the University of Kentucky (www.ca.uky.edu/refcig) and were conditioned between 7 and 21 d under controlled conditions at 22 ± 1 °C and relative humidity of 60 ± 3% according to ISO standard 3402 (International Organization for Standardization, 2010). They were smoked (55 ml puff over 2 s, twice a minute and 8 s pump exhaust time) on a 30-port carousel smoking machine (SM2000, Philip Morris, Int.). Reference cigarettes were smoked to standard butt length (i.e. approximately 35 mm).

Buccal and gingival tissues in triplicates were directly exposed at the air–liquid interface to the diluted mainstream CS from 3R4F or to 60% humidified air (sham/air-exposed controls) in the VITROCELL® exposure modules within a Climatic chamber (VITROCELL Systems GmbH, Waldkirch, Germany) at 37 °C. The CS was diluted with fresh air to 19.7 % (v/v) (low concentration) and 40.7% (v/v) (high concentration), the exposure duration was approximately 6–7 min per cigarette with 1 h rest between each cigarette (Figure 1). These dilutions correspond to nicotine concentrations of 0. 28 and 0.56 mg/L, respectively, according to the calibration of the VITROCELL® system (the amount of nicotine was determined using gas chromatography-flame ionization detection after trapping the aerosol by Extrelut 3NT columns (Merck, cat. # 115095), which were connected to an individual exhaust of the Dilution/Distribution system of the VITROCELL®). Based on a dose-range-finding study (data not shown), these CS concentrations induced less than 20% of cytotoxicity. After the exposure, the tissues were incubated with fresh culture medium immediately after exposure (0 h) or at 4, 24 and 48 h post-exposure, before further analyzed (Figure 1 and Supplemental Table S1). The applied procedure presented in Figure 1 is presumed to mimic the *in vivo* human tissues exposed to CS (i.e. a smoking situation).

Tissue toxicity and viability assays

Lactate dehydrogenase assay

Tissue cytotoxicity and cell viability were assessed in triplicate buccal and gingival tissue inserts. Samples of 50 µl cell culture basolateral medium were assayed 24 and 48 h after smoke exposure (post-exposure) using the CytoTox-ONE™ Homogeneous Membrane Integrity Assay (cat. # G7891, Promega, Dübendorf, Switzerland). The assay is based on the measurement of the release of LDH from cells with a damaged membrane. As a positive control test, the tissues were exposed for 2 h to 10% (v/v) Triton X-100 (cat. #93443-100 ml, Sigma-Aldrich, Buchs, Switzerland). The negative control test was done by measuring fresh culture medium.

Transepithelial electrical resistance assay

Tissue integrity at 48 h after smoke exposure was determined on three inserts per tissue type. Cellular TEER was measured using chopstick electrodes (STX-2) connected to an EVOM™ Epithelial Voltohmmeter (World Precision Instruments, Berlin, Germany) after the addition of 200 µl medium to the apical side of the tissues.

Histological and immunohistochemical analysis

At 0 and 48 h post-exposure to smoke, human buccal and gingival tissues were washed in PBS and fixed in 4% paraformaldehyde for 1 h and again washed twice with PBS. The fixed tissues were embedded in paraffin and subjected to histology and immunohistochemistry analysis. After paraffin embedding, four cross-sections were made from each tissue sample and mounted on a slide.

Histological analysis

A standard hematoxylin and eosin (H&E) staining was conducted. For the immunohistochemical staining, antigen retrieval was achieved by heating the sections on the slides in citraconic anhydride for 45 min at 98 °C. Afterwards, the tissue sections were incubated with primary antibodies for 1 h at 37 °C against p63 (1:150 dilution, cat # CM163B, BioCareMedical, Concord, CA) for the detection of basal cells, Ki-67 (1:600 dilution, cat # ab15580, AbCam, Cambridge, UK) for the detection of proliferating cells and human leukocyte antigen DR (HLA-DR; 1:1000 dilution, cat# Ab20181, AbCam) for the identification of Langerhans cells. The transcription factor, p63, is an established marker of basal cells and has been applied to identify both basal and suprabasal cells in buccal and gingival epithelia *in vivo* and *in vitro* (Chen et al., 2005; Hatakeyama et al., 2007; Marcelo et al., 2012; Terada et al., 2012; Westfall & Pietenpol, 2004). Ki67 is a nuclear antigen expressed in all phases of the cell cycle, except G0 and early G1, thus serving as a marker of proliferating epithelial cells (Yu et al., 1992), which are exclusively found among basal or suprabasal cells in oral epithelium (Dabija-Wolter et al., 2013; Dwivedi et al., 2013).

Quantification of stained cells

From each stained tissue, sample images were captured using confocal microscopy (Olympus FV1000 confocal microscope,

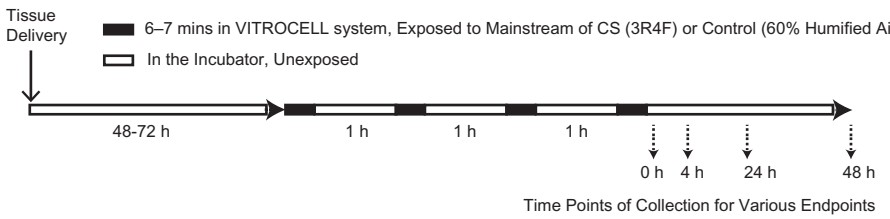

Figure 1. Experimental procedure of the smoke exposure.

Olympus America Inc., Center Valley, PA). From each stained tissue sample, the average number of stained cells and 4′,6-diamidine-2-phenylindole (DAPI)-positive cells in the epithelium were quantified on the three tissue cross-sections using Image J software (Bethesda, MD), and the percentage of specific antibody-stained cells in relation to the total number of DAPI-positive cells were calculated.

RNA isolation and microarray hybridization

Exposed tissues immediately after the last exposure (0 h) and at 4, 24 and 48 h post-exposure were washed twice with ice-cold PBS and lysed using QIAzol lysis reagent (miRNeasy Mini Kit cat #217004, Qiagen, Venlo, The Netherlands) and then frozen at −80 °C for up to 1 week. The miRNeasy Mini Kit was used to extract and purify mRNAs (including miRNAs). Total RNA was quantified using a NanoDrop ND1000 (Thermo Scientific, Waltham, MA) and its quality was verified by an Agilent 2100 Bioanalyzer (Agilent, Santa Clara, CA). A RNA Integrity Number (RIN) greater than 6 was required (the average of RIN in this study was 8.4). For mRNA analysis, 100 ng of total RNA were processed as described in the GeneChip HT 3′ IVT Express User Manual (Affymetrix). GeneChip Human Genome U133 Plus 2.0 Arrays were used for hybridization. RNA samples (3 µl × 33.3 ng/µl) were used for the Affymetrix DNA microarray. Randomization of samples had been achieved during the exposure of the tissues to CS, prior to the RNA extraction and microarray analysis.

Microarray data processing and analysis

Raw CEL files were background corrected, normalized and summarized using the GCRMA algorithm (Wu & Irizarry, 2005). Quality control of all chips was performed with R packages from Bioconductor (affy, affyPLM; Bolstad et al., 2003; Gautier et al., 2004). The log-intensities plot, Normalized Unscaled Standard Error (NUSE) plot, Relative Log Expression (RLE) plot, polyA controls boxplot, RNA degradation plot, spike-in controls boxplot, the pseudo image and raw image were generated for a QC check. Because outlier was not identified in these plots, all 70 CEL files passed the quality control process. Gene expression data were submitted to ArrayExpress with the following accession number: E-MTAB-2251. For every post-exposure time point, three biological replicates of both tissues for each concentration were available: R1, R2, R3 for sham, R*1, R*2, R*3 for the low concentration (19.7% CS) and R**1, R**2, R**3 for the high concentration (40.7% CS). To identify probe sets with a modulated expression on CS treatment, a linear model was defined as described below (Equation (1)). For every dose/treatment item/post-exposure (DTP), we fitted a model to the samples in the DTP group and the corresponding Sham group:

$$\text{Expression} = \beta_0 + \beta_1 \times \text{DTP} + \varepsilon, \quad (1)$$

The coefficients β_1 is equivalent to a pair-wise comparison, DTP – Sham (DTP). The doses did not fit in a single model because we expect strong heteroscedasticity between the dose and post-exposure variables. The coefficients β that represent the effects of interest described above was estimated using the Limma R package (Smyth, 2004).

Functional annotation analysis of the differentially expressed genes

Functional annotation of the differentially expressed genes (DEGs) from the *in vitro* and *in vivo* datasets was generated using the Database for Annotation, Visualization and Integrated Discovery (DAVID) analysis (Huang et al., 2009). The DEGs were analyzed using DAVID Functional Annotation Tool version 6.7. The ''KEGG Pathway'' category provided by DAVID was used to identify canonical pathways that were significantly associated with the DEGs. Pathways that satisfied the FDR <0.05 with at least two genes were selected and considered to be significantly associated with the datasets.

Comparative *in vivo/in vitro* enrichment analysis

To correlate between the effects of smoking on *in vivo* buccal mucosa samples (i.e. buccal samples of smokers versus non-smokers) and the effects of CS on *in vitro* buccal organotypic tissue cultures, we compared the gene expression profiles in the *in vivo* public dataset [smokers versus non-smokers, GSE17913 (Boyle et al., 2010)] to those generated from the *in vitro* buccal organotypic culture over various post-exposure time-points of CS at the different concentrations. Gene-set analysis (GSA) was performed for all estimated effects (Efron & Tibshirani, 2007). The two-sample *t*-statistic Zi was chosen for the gene level statistics; the ''maxmean statistic'' rather than the Kolmogorov–Smirnov statistics was chosen for the gene set enrichment analysis (GSEA) (Subramanian et al., 2005) because maxmean statistic is shown to be more reliable than the Kolmogorov–Smirnov statistics that is used in GSEA (Ackermann & Strimmer, 2009). Both gene sampling and label permutation tests were used to test gene set significance. Gene set scores with an associated false discovery rate (FDR) <0.05 were considered to be statistically significant. The heatmaps were generated using the heatmap.2 function in the ''gplots'' R package (Warnes et al., 2012). The row hierarchical clustering was performed using the hclust function in the ''stats'' R package (R Development Core Team, 2010) with a complete agglomeration and Euclidean distance metrics.

Calculation of the exposure-impact on biological processes using network-based systems biology approach

Transcriptomic data were analyzed in the context of hierarchically structured network models describing the molecular mechanisms underlying essential biological processes in non-diseased lung cells (Hoeng et al., 2012). Table 1 lists all of the network models and their subnetworks that were applied for the analysis.

The effects of exposure were quantified by scoring the impact on each subnetwork (referred to as ''network perturbation amplitude'', NPA; Martin et al., 2012). The NPA values were calculated using the Geometric Perturbation Index (GPI) metric, and accounting for the overlap between

Table 1. Network models and subnetworks applied for the computational analysis of network perturbation amplitudes (NPAs) and biological impact factor (BIF).

Network model	Subnetwork	References
Cell cycle	Cell cycle	Thomson et al. (2013) Westra et al. (2011)
Regulation of proliferation	Calcium Cell interaction Clock Epigenetics Growth factor Hedgehog Hox Jak Stat Mapk Notch Nuclear receptors PGE2 Wnt mTor	Thomson et al. (2013) Westra et al. (2011)
Pulmonary inflammation (inflammatory process)	Epithelial cell barrier defense Epithelial proinflammatory signaling Tissue damage Dendritic cell activation (applicable for the buccal tissue) Dendritic cell migration to tissue (applicable for the buccal tissue) Dendritic cell migration to lymph node(applicable for the buccal tissue)	Westra et al. (2013)
Stress	Xenobiotic/Drug metabolism response Endoplasmic reticulum stress Hypoxic stress NFE2L2 signaling Osmotic stress Oxidative stress	Schlage et al. (2011)
Apoptosis	Caspase cascade ER stress-induced apoptosis MAPK signaling NFkB signaling PKC signaling Proapoptotic mitochondrial signaling Prosurvival mitochondrial signaling TNFR1_Fas signaling TP53 TS	Gebel et al. (2013)
DNA damage	Components affecting TP53 activity Components affecting TP73 activity Components affecting TP63 activity DNA damage to G1/S checkpoint DNA damage to G2/M checkpoint Double-strand break response Inhibition of DNA repair Single-strand break response TP53 TS	Gebel et al. (2013)
Necroptosis	Fas activation Proinflammatory mediators RIPK/ROS mediated execution TNFR1 activation	Gebel et al. (2013)
Autophagy	ATG induction of autophgy Autophagy induction mTOR signaling Protein synthesis	Gebel et al. (2013)
Senescence	Regulation by tumor suppressors Oncogene induced senescence Replicative senescence Stress induced premature senescence Transcriptional regulation of the SASP	Gebel et al. (2013)

subnetworks by network scoring using the Downweighting of Promiscuous Hypotheses method (Thomson et al., 2013). Two companion statistics are associated with every network score: Uncertainty statistics and Specificity statistics. The uncertainty statistics is the 95%-confidence interval accounting for the variation between biological replicates, whereas the specificity statistics tests whether the NPA value is greater (in absolute value) than any score obtained when replacing the genes underlying the network with randomly chosen genes (Martin et al., 2012). The p value threshold of the specificity statistic is set to 0.05. Normalized NPA values are computed as the Z-scores with respect to the values obtained from the specificity calculation (Gonzalez-Suarez et al., 2014). The NPA value of a network can be significant without having all of its subnetworks being significant.

In addition to the impact/perturbation scores at the levels of network and subnetwork, the effects of the CS exposure were further quantified as a system-wide metric for biological impact – the biological impact factor (BIF; Hoeng et al., 2012; Thomson et al., 2013). This positive value of BIF summarizes the impacts of the exposure on the cellular system into a single number, thus enabling a simple and high-level comparison of the treatment effects across various post-exposure time-points and tissues. The calculation of the BIF required the complete collection of hierarchically structured network models from Table 1 and entailed in aggregating the (non-normalized) NPA values of the individual networks as described before (Thomson et al., 2013).

Measurement of pro-inflammatory mediators

The released pro-inflammatory mediators were measured at 24 h after smoke exposure in the basolateral medium of EpiOral™ and EpiGingival™ tissue cultures (in 100 µL medium stored at −80 °C). Secretion of granulocyte-colony stimulating factor (G-CSF), granulocyte macrophage-colony stimulating factor (GM-CSF), interferon gamma inducible protein 10 (IP-10), interleukin (IL)-1α, IL-1β, IL-6, IL-8, monocyte chemoattractant protein-1 (MCP-1), vascular endothelial growth factor (VEGF), eotaxin, regulated on activation, normal T cell expressed and secreted (RANTES) (Milliplex MAP Human cytokine/chemokine magnetic bead panel, HCYTOMAG-60K, Millipore) and MMP-1 and MMP-9 (Milliplex MAP Human MMP magnetic bead panel 2, HMMP2MAG-55K, Millipore) were measured by Luminex-based technology following the technical recommendations of Milliplex (Millipore). As a positive control test, the buccal and gingival tissues ($N = 3$ inserts/tissue) were treated with a combination of tumor necrosis factor (TNF)-α + IL-1β in the basolateral medium, for 24 h at 37 °C and 5% CO_2 (data not shown).

The results from the Luminex analysis were plotted as a heatmap. For comparison, the differential expression of the genes at the time points at 0, 4 and 24 h post-exposure that correspond to those measured by Luminex were plotted in the same format using the following approach: fold changes were obtained by taking the log2 ratio of the cytokine abundance or of the gene expression between the CS and air-exposed groups for the two tissues. Welch's t-test was performed to test the null hypothesis that the cytokine abundance or the log2-based gene expression between the CS exposed groups (for each of the concentrations: 19.7 and 40.7%) and air-exposed groups were the same. Fold change was set as zero for the p values >0.05. Blue and red indicate negative and positive fold changes, respectively. The heatmaps were generated using the heatmap.2 function in the ''gplots'' R package (Warnes et al., 2012). The hierarchical clustering was performed using the hclust function in the ''stats'' R package (R Development Core Team, 2012).

Measurement of CYP1A1/CYP1B1 activity

CYP enzyme activity was measured at 48 h post-exposure in the basolateral medium of the EpiOral™ and EpiGingival™ tissues using non-lytic P450-Glo™ assays (CYP1A1/CYP1B1 assay cat #: V8752; Promega) based on luminescence following the manufacturer's recommendations (P450-Glo assay technical bulletin, Promega). Tissues were incubated in medium with luminogenic CYP-Glo substrate, i.e. luciferin-CEE for 3 h (targeting both CYP1A1 and CYP1B1), to generate a luciferin product that was quantified in the supernatant by a light-generating reaction upon the addition of luciferin detection reagent. As a positive control test, tissues were treated by 30 nM 2,3,7,8-tetrachlorodibenzo-p-dioxin (TCDD) that was added to the basolateral medium for 48 h at 37 °C and 5% CO_2 (new treatment was administered every 24 h) prior to the collection of the medium for the measurement of CYP activity.

Results

Cytotoxicity and tissue integrity

LDH release

Cell viability was assessed by measuring the levels of LDH released in the cultured basolateral medium at the various post-exposure time-points. In the buccal tissues, both concentrations of CS did not cause a significant increase of LDH release at all post-exposure time-points at 0, 4, 24 and 48 h (Figure 2A). In the gingival tissues (Figure 2B), one condition (19.7 % CS at 4 h post-exposure) resulted in a statistically significant increase in LDH release.

Epithelial permeability

TEER assay was used to determine the integrity of the epithelial barrier function and to examine the gross epithelial damage at the 48 h post-exposure period. The buccal tissues exposed to 19.7 and 40.7% CS had increased TEER mean values ±SEM ($\sim 2000 \pm 200$ and $\sim 3500 \pm 700\ \Omega\,cm^2$, respectively) as compared to the air-exposed control ($\sim 1400 \pm 100\ \Omega \times cm^2$; Figure 2C). Similarly, the gingival tissues exposed to 40.7% CS had increased TEER values ($\sim 2700 \pm 400\ \Omega\,cm^2$) as compared to the sham control ($\sim 2200 \pm 500\ \Omega\,cm^2$) (Figure 2D). The increase of TEER in the gingival tissues exposed to the lower concentration of CS was not statistically significant as compared to the air-exposed control. The positive control test upon treatment of the detergent Triton X-100 completely diminished their epithelial barrier function ($<\sim 100\ \Omega\,cm^2$), whereas PBS treatment to both tissues yielded the same values as the air-exposed control groups (Figure 2C and D).

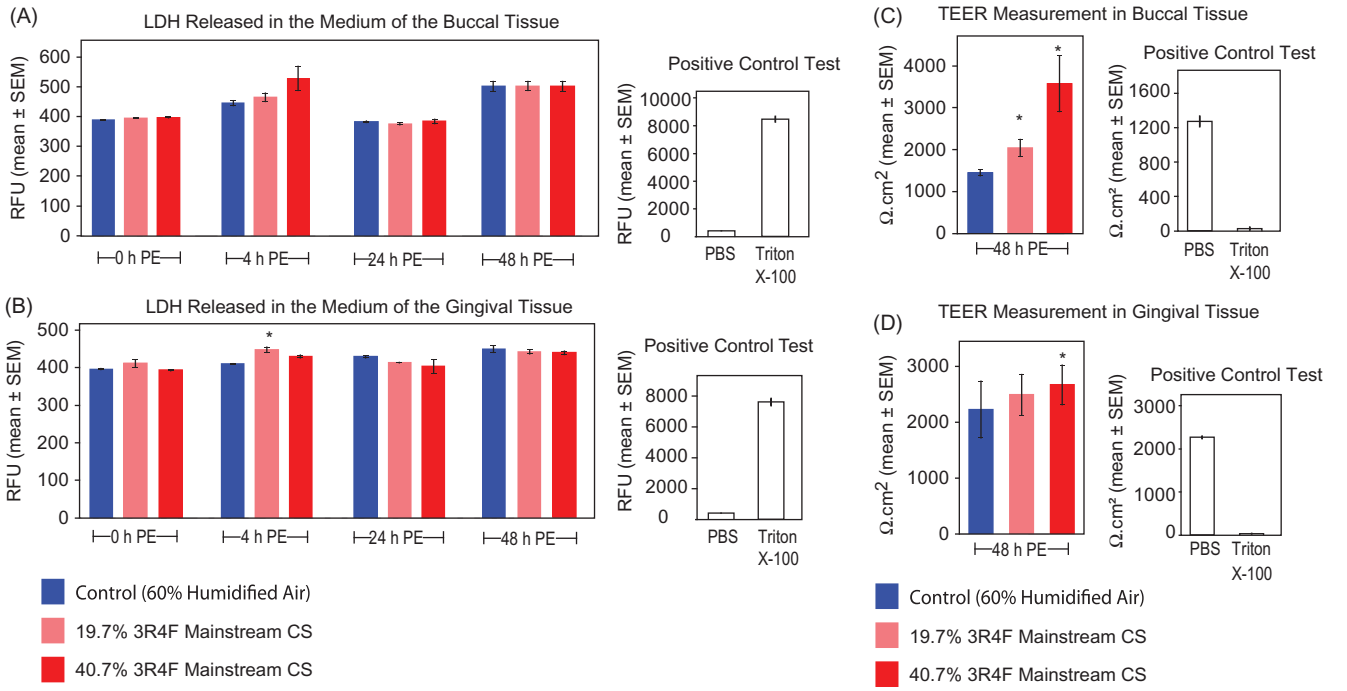

Figure 2. Tissue viability and epithelial barrier function assessment. LDH activity was measured in the culture medium immediately after exposure (0 h), and at 4, 24 and 48 h PE of CS of the buccal (A) and gingival (B) tissue cultures. TEER was measured at 48 h PE to CS in buccal (C) and gingival (D) tissue cultures. The charts on the right show the positive control tests using Triton X-100 treatment. Means ± SEM are shown ($N = 3$ inserts following a single exposure run). Asterisk indicates significant $p < 0.05$ compared with the air-exposed control within each of the post-exposure time-point, Dunnett adjusted for multiple comparison. Abbreviations: CS, cigarette smoke; LDH, lactate dehydrogenase; PE, post-exposure; RFU, raw fluorescence unit; TEER, transepithelial electrical resistance; SEM, standard error of the mean.

Tissue integrity

Tissue integrity was further assessed using histological examination. Analyses of the H&E-stained tissue sections did not reveal obvious morphological/structural changes in the CS-exposed buccal and gingival tissues, although a slight increase in epithelial thickness was observed in the tissues exposed to the higher concentration of CS, as compared with the air-exposed controls at 48 h post-exposure (Figure 3A).

Immunohistochemical identification of cell types and proliferative state

In the buccal tissues, the proportions of p63-stained cells – a marker of basal cells – were significantly decreased with the increasing concentrations of CS (Figure 3B). The proportions of Ki67-stained cells – a marker of proliferating epithelial cells, which were observed exclusively in the basal cell layers – were not significantly different among all groups (Figure 3B). The fraction of Langerhans cells, which was indicated using a surface marker expressed by antigen presenting cells (i.e. HLA-DR staining), only presented in the buccal tissues. The proportion of HLA-DR-stained cells was not different among all groups, although a declining trend of HLA-DR-staining in a CS concentration-dependent manner was observed (Figure 3B).

In the gingival tissues (Figure 3C), the proportions of p63-positive cells were not statistically different among the groups. The proportions of Ki67-stained cells were reduced in the CS-exposed tissues without a dose-response effect (Figure 3C). HLA-DR staining was not performed on the gingival tissues because the tissue models were developed without Langerhans cells. Interestingly, the proportions of p63-stained cells in the air-exposed gingival tissue were comparable to the buccal tissue, whereas for the Ki67-positive cells, the proportions were approximately twice that of the buccal tissues (Figure 3C).

Transcriptomic data evaluation

Enrichment of canonical pathways

Pathway annotation (DAVID analysis) identified a small number of enriched canonical pathways (KEGG pathways, FDR <0.05) from the differentially regulated genes (DEGs) of the buccal and gingival tissues exposed to the higher concentration of CS (40.7%). The pathway annotations were more extensive in the upregulated DEGs (Figure 4).

For the buccal tissues, ''Steroid hormone biosynthesis'' and ''Metabolism of xenobiotics by P450s'' pathways were identified to be significantly enriched in the dataset generated from the tissues at the 24 h post-exposure to 40.7% CS (Figure 4A). At the 48 h post-exposure, ''Ribosome'' pathway was significantly associated with the downregulated DEGs. For the gingival tissues, ''Steroid hormone biosynthesis'' and ''Metabolism of xenobiotics by P450s'' were significantly upregulated at the 4, 24 and 48 h post-exposure time points following the 40.7% CS exposure (Figure 4B). Supplemental Table S2 lists all annotations generated using DAVID along with the associated genes.

Biological-network approach analysis

The network-based systems biology approach was used to further assess the transcriptomic data from the tissues exposed to the higher concentration of CS (40.7%). The whole-systems impacts are expressed as BIF (see ''Materials and methods''

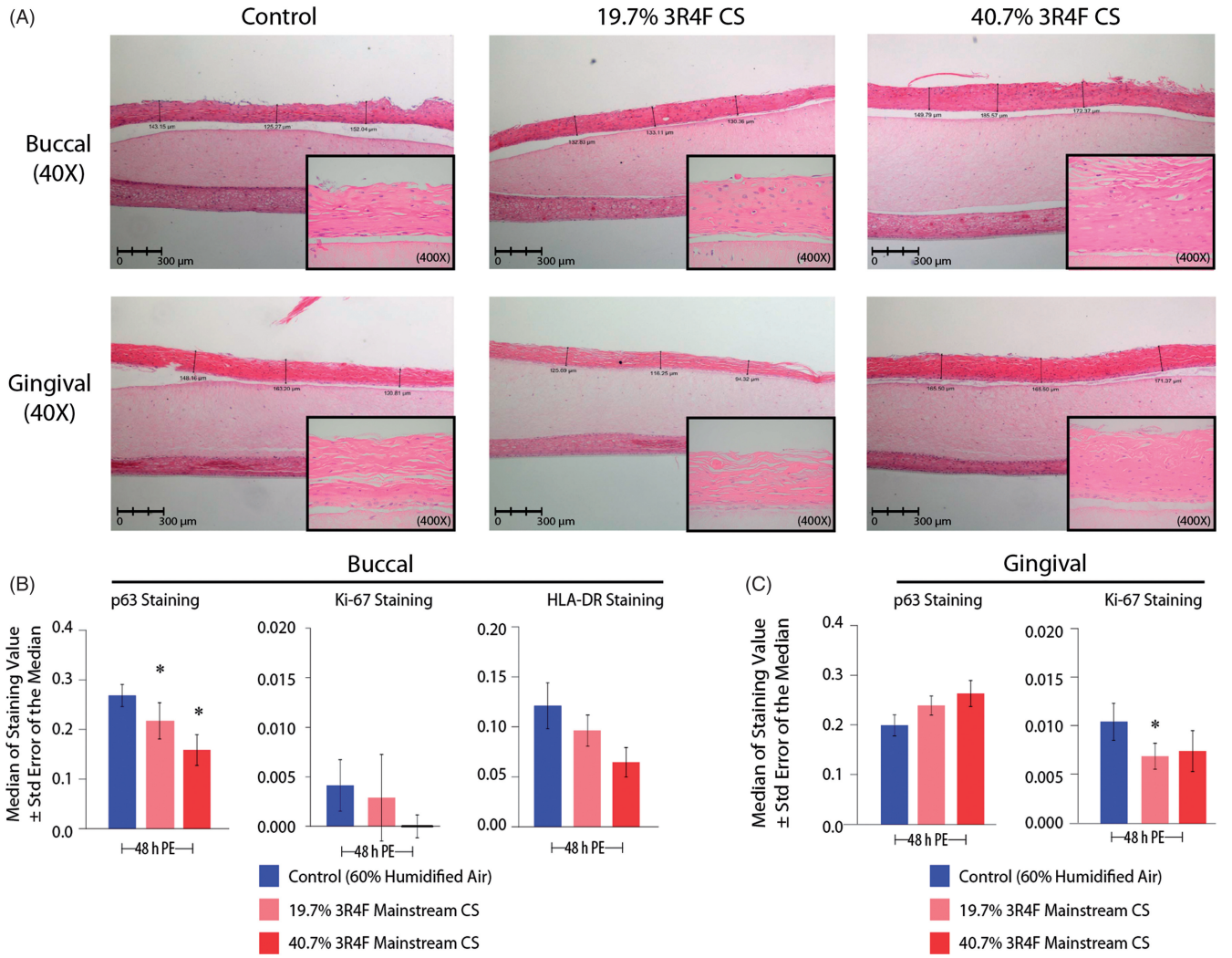

Figure 3. Histological examination of tissue structure and immunohistochemical identification of cell types and proliferation. H&E staining (40×) of the buccal (upper panels) and gingival tissues (lower panels) are shown in (A) at 48 h PE to CS at 19.7 and 40.7% compared with the air-exposed control. Insets show a 400× magnification. Quantification of immunostaining in the buccal (B) and gingival (C) tissues for various markers was performed. Basal cells (p63), proliferating basal cells (Ki-67) and a surface marker expressed in antigen presenting cells (HLA-DR, only in B) are shown as the ratios of immunostained cells per total cell count (number of DAPI-positive cells). Medians ± standard error of the medians are shown ($N = 3$ inserts following a single exposure run). Asterisk indicates significant $p < 0.05$ compared with the air-exposed control. Abbreviations: CS, cigarette smoke; DAPI, 4′,6-diamidino-2-phenylindole; H&E, hematoxylin & eosin; HLA-DR, human leukocyte antigen DR; PE, post-exposure.

section; Figure 5), which reflect the overall impact (perturbation) levels in the tissues-exposed to the higher concentration of CS (40.7%) as compared to the air-exposed tissues (Figures 5 and 6). Greatest systems impact of CS was observed at the 4 h post-exposure time-point in both tissues (Figure 5).

The BIF calculation takes into account the individual biological mechanisms (represented and built as biological networks, Table 1). Quantitatively, the impacts on each of the mechanisms were expressed as the normalized NPA values, which enable comparisons among the different networks at a given post-exposure time-point, which were plotted as spider graphs (Figure 5B–E). For each of the post-exposure time-points, significant impacts on Stress and Senescence were observed.

The biological network models are hierarchically structured, reflecting biological mechanisms relevant to respiratory system toxicity (Hoeng et al., 2012; Thomson et al., 2013). Because the network hierarchy is composed of subnetworks, to uncover more detailed mechanisms affected by CS exposure, we investigated the biological processes that are represented at the level of the subnetworks (Table 1). Figure 6 illustrates the breakdown of the before-mentioned perturbed networks to their subnetworks. The degree of the exposure impacts is quantitatively described as a normalized NPA (see ''Materials and methods'' section). Within the Stress network (Figure 6A and B), the Xenobiotic Metabolism and the Nuclear factor (erythroid-derived 2)-like 2 (NFE2L2, also known as Nrf2) subnetworks were highly impacted in a similar manner (Figure 6B). However, the Oxidative Stress subnetwork was impacted only in the gingival tissues at 4 and 48 h post-exposure time-points (Figure 6B). Within the Pulmonary Inflammation network (Figure 6C and D), the Epithelial Barrier Defense subnetwork was significantly affected in both tissues at 4 h post-exposure only. Furthermore, within the Necroptosis network, significant impacts were detected for subneworks Fas Activation and Tumor necrosis factor receptor 1 (TNFR1) Activation (Figure 6F). The results of the NPA analysis from all of the

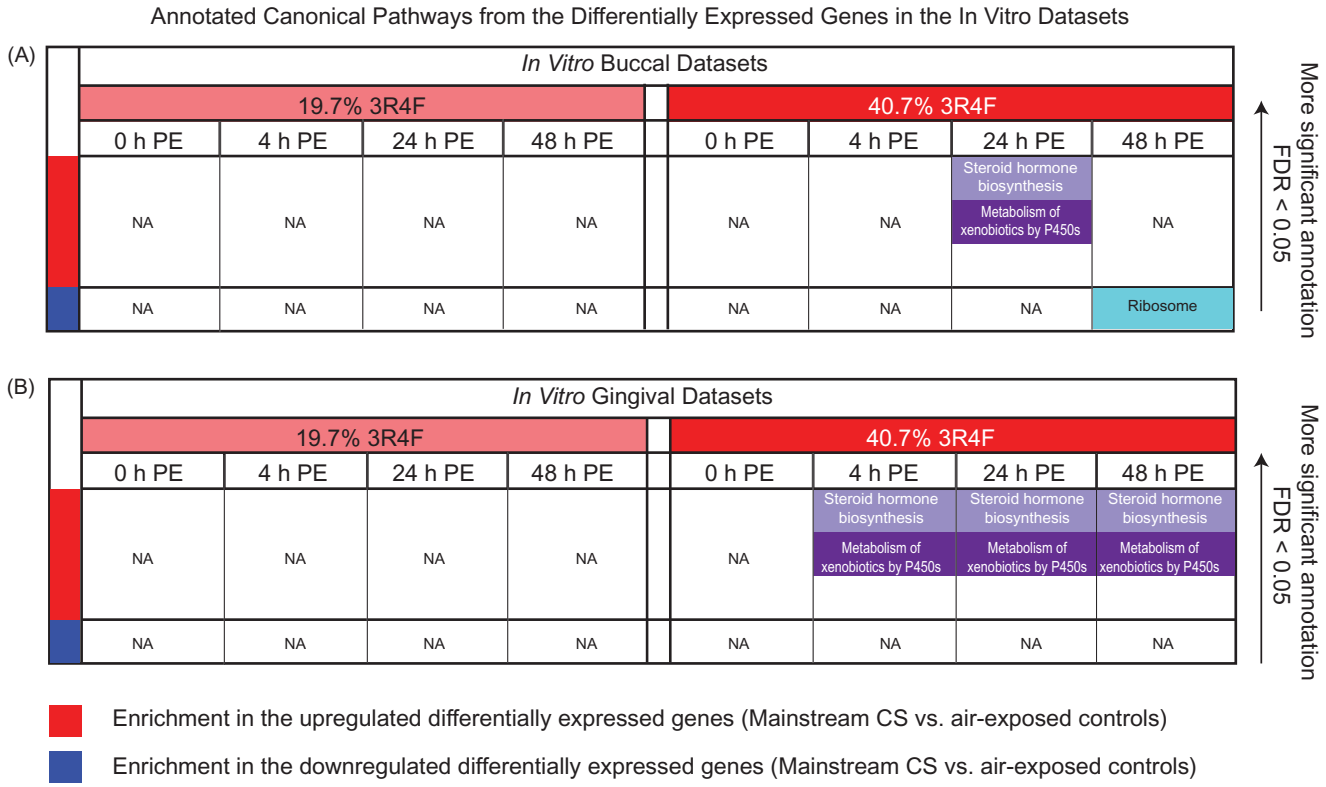

Figure 4. Enriched canonical pathways in the *in vitro* datasets. Significant canonical pathways (in different colors) were extracted from the differentially expressed genes in the buccal and gingival organotypic tissue cultures at various time-points of PE to CS (19.7 and 40.7%) compared with the air-exposed control using DAVID annotation tools (FDR < 0.05, with at least two gene count in the annotation). NA indicates no significant enrichment was identified using the before-mentioned threshold. All annotations and associated genes within each of the canonical pathways are listed in Supplemental Table S2. Abbreviations: CS, cigarette smoke; FDR, false discovery rate; NA, not available; PE, post-exposure.

networks along with their subnetworks used for the analysis are displayed in Supplemental Figure S1.

Comparison of in vitro *versus* in vivo *buccal epithelial signatures of exposure to CS*

Similar to the above approach, the impact of exposure observed in the *in vitro* buccal tissue exposed to CS were compared to buccal epithelial samples of smokers. Because an *in vivo* public dataset containing gene expression profiles of smokers and non-smokers was not available for gingival samples, we only conducted a comparative *in vivo/in vitro* analysis of the buccal tissue. The public dataset GSE17913 (Boyle et al., 2010) containing gene expression profiles from buccal biopsies of smokers and non-smokers, was used to assess the responses to CS exposure *in vivo*. Figure 7(A–D) illustrates the comparability of the *in vivo/in vitro* datasets in the context of biological network models. Consistent significant impacts on the Stress network were observed in both *in vivo* and *in vitro* datasets (Figure 7). Within the Stress network, significant impacts on the Xenobiotics Metabolism subnetwork were detected (Supplemental Figure S1).

Furthermore, a comparative enrichment analysis (see ''Materials and methods'' section) was conducted to compare the pathways annotations (DAVID) between those generated from the transcriptomics data derived from the buccal organotypic tissues (*in vitro*) and those from the published buccal mucosa biopsies dataset GSE17913 (*in vivo*; Boyle et al., 2010; Figure 7E). Enrichment scores and a heatmap of the up- and down-DEGs are presented in Supplemental Figure S2. Consistently, in both the *in vitro* and *in vivo* samples, ''Metabolism of xenobiotics by P450s'' and ''Steroid hormone biosynthesis'' pathway annotations were identified from all of the post-exposure time-points dataset (except for buccal tissues exposed to the lower concentration of CS at the 0 and 48 h post-exposure; Figure 7E). Many of the genes of phase I and II enzymes, including *CYP1A1*, *CYP1B1*, *AKR1C* isoforms, *ALDH3A1*, *PTGES*, *GPX2*, *GSTM3* and several *UGT* isoforms were significantly associated with these annotations (Supplemental Table S3). In addition, ''Arachidonic metabolism'' was annotated at the earlier post-exposure time points for the tissues exposed to the lower concentration of CS (19.7%; i.e. at 4 and 24 h) than those exposed to the highest concentration of CS (40.7%; i.e. 24 and 48 h).

Activity of the cytochrome P450 CYP1A1/CYP1B1

Both buccal and gingival tissues had basal activities of CYP1A1/1B1 enzyme that were measured at 48 h post-exposure (Figure 8A and B). CYP1A1 and CYP1B1 have been shown to metabolize tobacco smoke constituents (Port et al., 2004). Tissues exposed to 19.7% CS, had increased levels of CYP1A1/1B1 activity, although the increase in the buccal tissues could not reach statistical significance (Figure 8A and B). The activities of the CYP1A1/1B1 were not altered in both tissues exposed to the higher concentration of CS as compared to the air-exposed tissues.

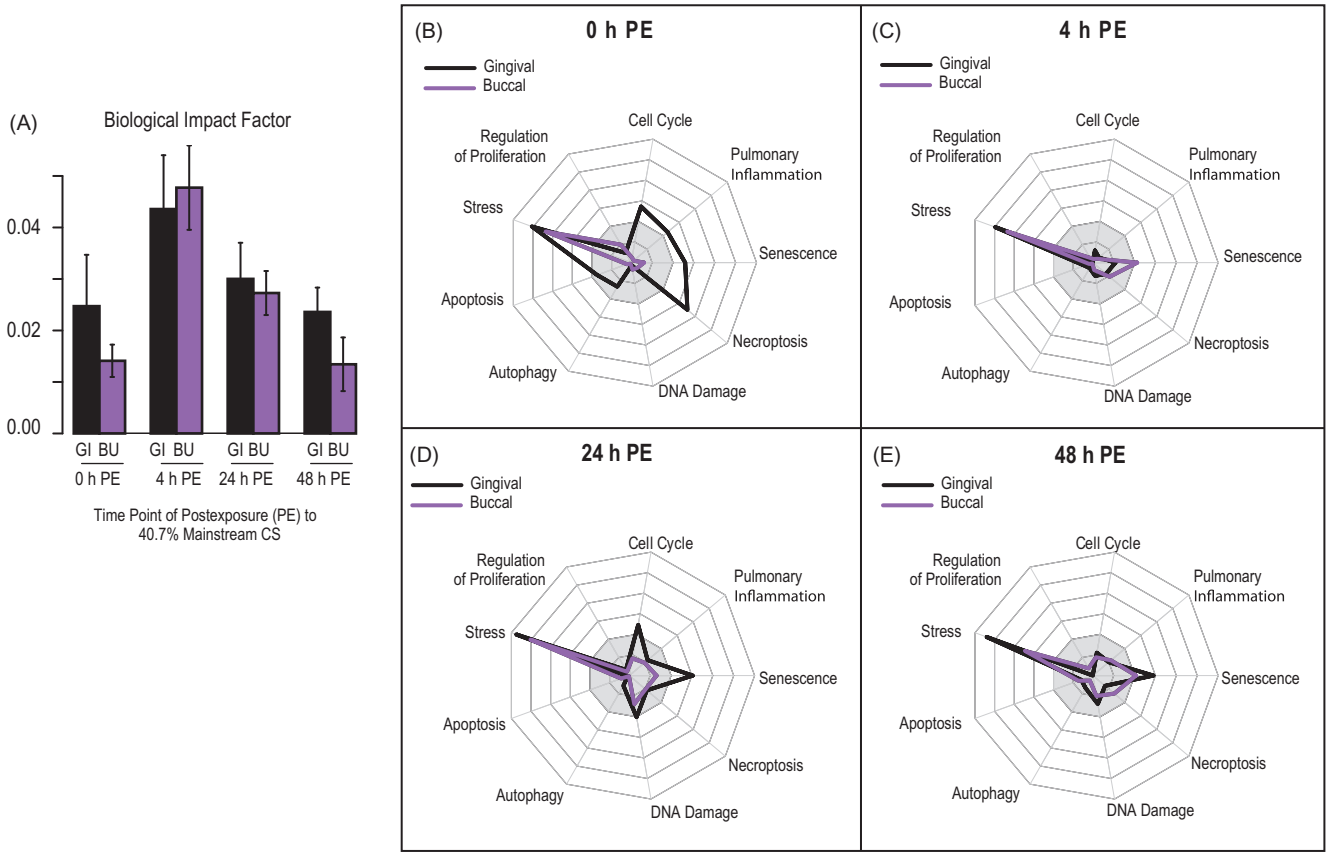

Figure 5. Transcriptomic analysis using a network-based biological impact factor analysis. The overall biological impact calculated as biological impact factor (BIF) from all aggregated biological network models is shown in (A) for the various PE time-points following exposure to 40.7% CS in the gingival (GI) and buccal (BU) tissues. (B)–(E) show spider plots that display the normalized NPA values illustrating the quantification of the impacted biological networks for each of the post-exposure time-points. Gray areas in the center of the spider plots indicate statistically non-significant perturbation of the different networks according to the Specificity statistics, refer the ''Materials and methods'' section. Abbreviations: CS, cigarette smoke; PE, post-exposure.

Inflammatory mediator secretion

To determine the effects of CS on the secretion of inflammatory mediators following exposure, the levels of cytokines, chemokines and other inflammatory mediators were determined in the culture medium at 24 h post-exposure to CS. Figure 8(C) shows the levels of all of the measured inflammatory mediators in the CS-exposed tissues as compared to the air-exposed tissues. Increased secretion of MMP-1 and VEGF protein was observed in both tissues exposed to CS (Figure 8C). Moreover, decreased levels of IP-10 were found in both tissues exposed to the 40.7% CS. In addition, only in the buccal tissue, increase of IL-1β (for the 40.7% CS), IL-6 and G-CSF (for the 19.7% CS) were observed.

To correlate the levels of these secreted proteins – which were measured at 24 h post-exposure – to the corresponding gene expression, we plotted a heatmap of the differential gene expression derived from the 0, 4 and 24 h post-exposure time-points (Figure 8D). In agreement with the levels of secreted proteins, the levels of *MMP1* gene expression were found to be increased in both tissues at all these post-exposure time-points, despite mostly occurring only in the tissues exposed to the 40.7% CS (Figure 8D). On the other hand, the levels of *IL1A* and *IL1B* gene expression were found to be increased in both tissues at all the post-exposure time-points (Figure 8D), which were different from their protein levels (Figure 8C).

Discussion

Weak effects of CS exposure on tissue integrity, cellular structure and cytotoxicity

The results suggest that the oral tissue models elicit a weak adaptive response; this observation is more noticeable for the buccal tissues, in which significant increase of TEER was observed following the CS exposure. This is also supported by the marked activation of the Epithelial Cell Barrier Defense subnetwork (Supplemental Figure S1) and by a slight increase of epithelial thickness in the histological sections of the tissues. The decreased number of p63-stained cells in the CS-exposed buccal tissues, which suggested an increased rate of differentiation of the basal cells, also supported this assumption. For example, increased squamous differentiation and cornification are known to be part of an adaptive response (Mezentsev & Amundson, 2011). Moreover, a relatively weaker increase of TEER values was observed in the CS-exposed gingival tissues as compared to those in the buccal tissues. This observation is supported by the modest increase of epithelial thickness in the CS-exposed gingival tissue without significant alterations of the proportion of the p63-stained cells, as well as with the weaker impact of the activation on the Epithelial Cell Barrier Defense subnetwork in the gingival as compared to the buccal tissues (Supplemental Figure S1).

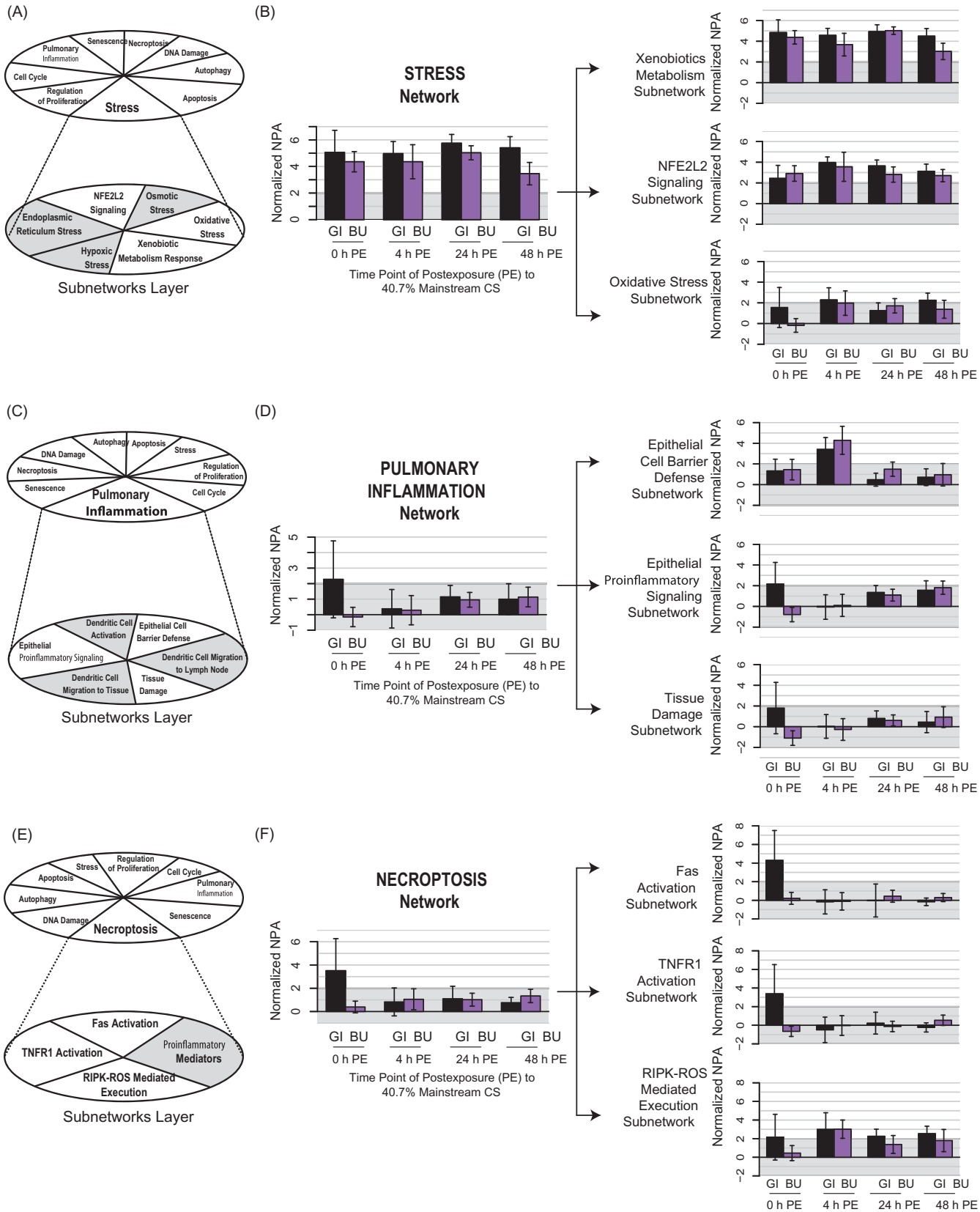

Figure 6. Perturbation of various biological networks and subnetworks upon 40.7% CS exposure in the gingival (GI) and buccal (BU) tissues. Illustration of the decomposition of Stress network (A), Pulmonary Inflammation network (C) and Necroptosis network (E) into their subnetworks. Gray areas in the illustration indicate the subnetworks that were not significantly perturbed. Normalized NPA values indicated the levels of impact on the biological processes designated as Stress, Pulmonary Inflammation and Necroptosis networks and their subnetworks are shown in B, D and F, respectively. Bar charts above the gray area, those that were statistically significantly impacted (described in the ''Materials and methods'' section). Abbreviations: NPA, network perturbation amplitude, TNFR1, tumor necrosis factor receptor 1; RIPK-ROS, receptor-interacting serine/threonine-protein kinase-reactive oxygen species.

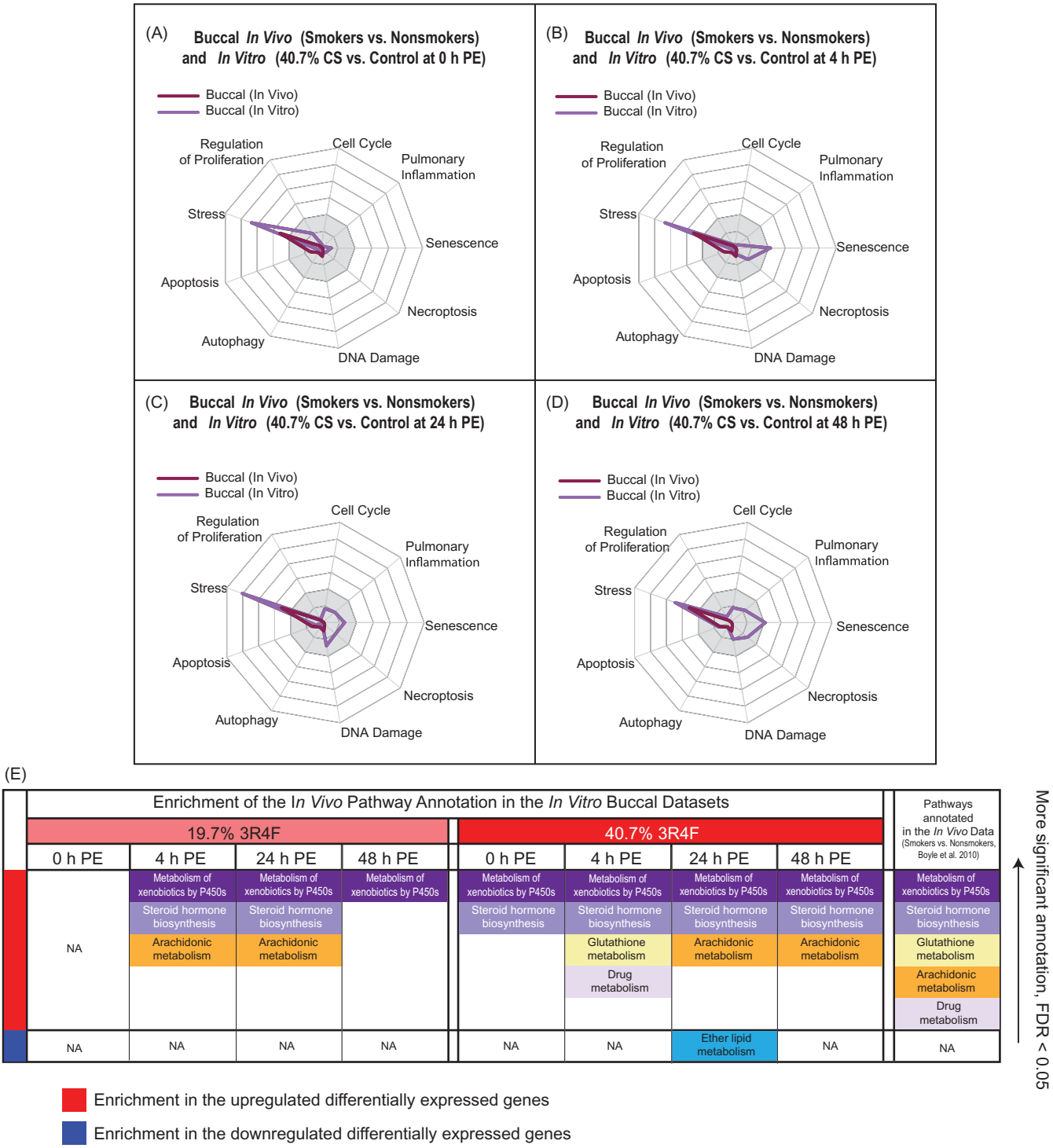

Figure 7. Comparability of the gene expression changes *in vivo* to the *in vitro* buccal samples upon exposure to CS. The comparison of the responses to CS exposure *in vivo* derived from buccal epithelial cells of smokers (GSE17913; Boyle et al., 2010) and that of *in vitro* buccal epithelium exposed to CS at various time-points of post-exposure illustrated in spider plots using the network-based approach (A–D, with the same conventions as described for Figure 5A–D). Gray areas in the center of the spider plots indicate non-significant perturbation of the different networks. E shows the annotated canonical pathways (DAVID) extracted from the leading genes derived from the comparative enrichment analysis with FDR < 0.05, with at least two gene count in the annotation (Comparative enrichment scores are shown in Supplemental Figure S2). Red and blue bars indicate the enrichment scores of the upregulated and downregulated genes, respectively, derived from the *in vivo* data that were enriched with the *in vitro* datasets. All annotations and associated genes within each of the canonical pathways from DAVID are listed in Supplemental Table S3. N/A indicates no significant enrichment was identified using these thresholds. Abbreviations: CS, cigarette smoke; NA, not available; PE, post-exposure.

Although the increase of LDH release in the gingival tissues exposed to 19.7% CS at 4 h post-exposure was statistically significant (Figure 2B), we questioned the biological significance because of the lack of a dose-response effect. As compared to the positive control Triton X-100, which had a RLU value of 7800 reflecting 100% of the cells were damaged, the increase of LDH release in the CS-exposed gingival tissue would only indicate roughly less than

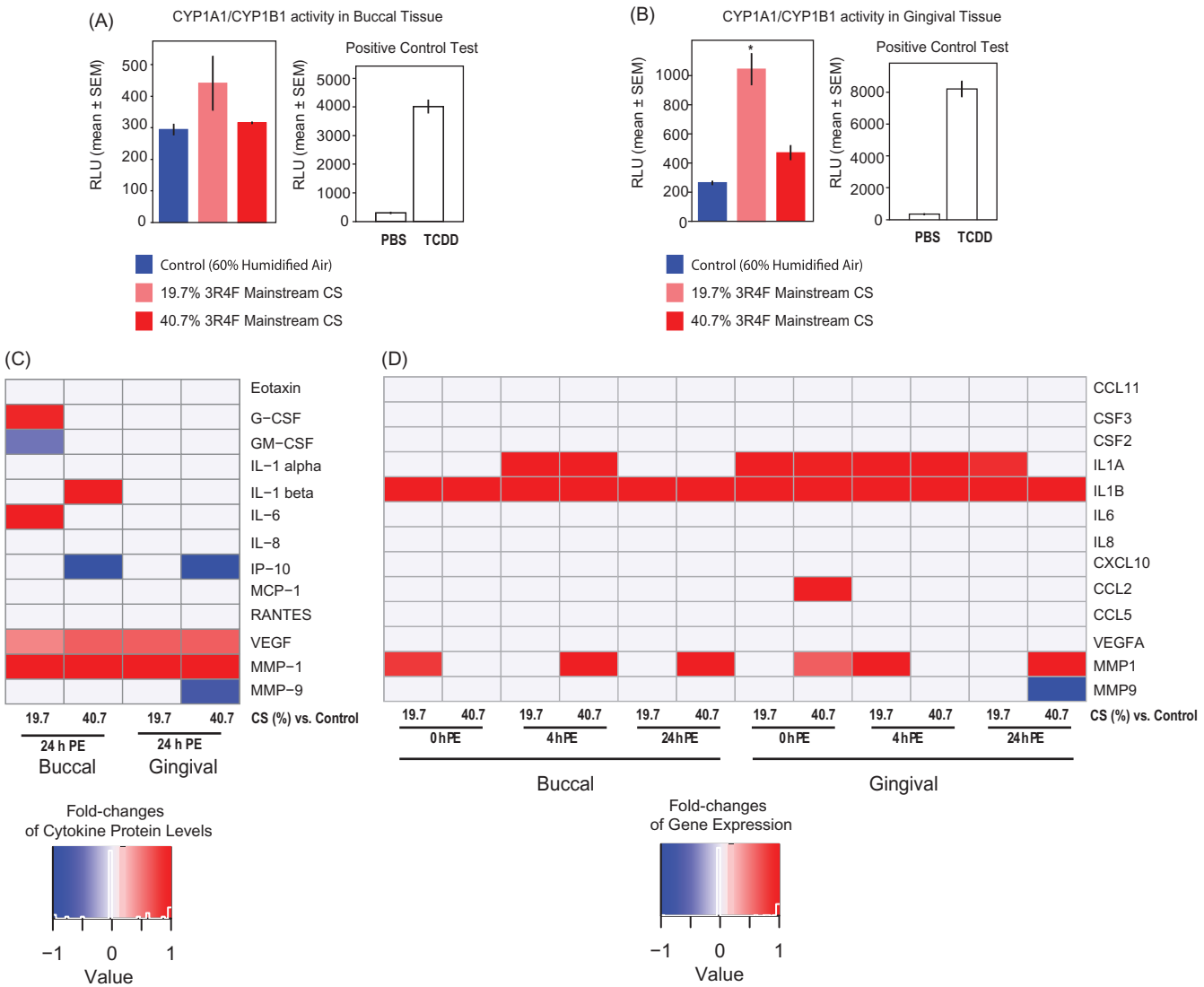

Figure 8. CYP1A1/1B1 enzyme activity and cytokine secretion in buccal and gingival tissues. Activity levels of CYP1A1/1B1 were measured at 24 h post-exposure to CS (17.9 and 40.7%) in the buccal (A) and gingival (B) tissues ($N = 3$ inserts following a single exposure run). Positive control tests are shown (right side of each panel) using TCDD as an inducer of CYP1A1/1B1 activity. Inflammatory mediators (C) and the corresponding gene expression (D) were measured at 24 h post-exposure of CS compared with the air-exposed tissues ($N = 3$ inserts following a single exposure run). Columns are representing different tissues as indicated in the label under the heatmap. Fold changes were obtained by taking the log2 ratio of the cytokine abundance (C) or of the gene expression (D) between the CS group and air-exposed exposure group for every tissue. Welch's *t*-test was performed to test the null hypothesis that cytokine abundance (C) or log2-based gene expression (D) in the CS (19.7 and 40.7%) groups and air-exposed group was equivalent. Fold change was set to be zero for the $p > 0.05$. Blue and red colors indicate negative or positive fold-changes in the CS-exposed tissues as compared to the air-exposed tissues, respectively. Abbreviations: CCL, CC chemokine ligand; CS, cigarette smoke; CYP, cytochrome; G-CSF, granulocyte-colony stimulating factor; GM-CSF, granulocyte macrophage-colony stimulating factor; IL, interleukin; IP-10, interferon gamma inducible protein 10; MCP-1, monocyte chemoattractant protein-1; MMP, matrix metalloproteinase; SEM, standard error of the mean; RANTES, regulated on activation, normal T cell expressed and secreted; RLU, raw luminescence unit; TCDD, 2,3,7,8-tetrachlorodibenzo-*p*-dioxin; VEGF, vascular endothelial growth factor; PE, post-exposure.

15–20% of the cells that were damaged. Moreover, other measured endpoints (i.e. TEER, histology analyses) did not suggest significant toxicity of the 19.7% CS to the gingival tissues. In addition, our results indicated that CS exposure did not affect the levels of proliferating cells in both tissues as indicated by the proportions of Ki67-stained cells (despite a decreasing trend of Ki67-stained cells upon CS exposure in both tissues). This is in contrast with that observed in tongue epithelium exposed to acetaldehyde, a constituent of tobacco smoke. Homann et al. (1997) reported that the acetaldehyde exposure increased the number of Ki67-stained cells in the rat tongue epithelium. This discrepancy could be explained by the different proliferating capacity between the different oral mucosa types in mammals (Rowat & Squier, 1986), such as the different proliferating capacity among the three major subtypes: masticatory (hard palate and gingiva), specialized (dorsal surface of the tongue) and lining (buccal mucosa, ventral surface of the tongue, soft palate and intra-oral surfaces of the lips and alveolar mucosa; Jones & Klein, 2013).

Our study also indicated that the oral tissue models had lower sensitivity to CS exposure. In this study, the concentrations of 19.7 and 40.7% were used to examine the effects of CS exposure, which did not cause obvious toxic effects (based on the results of LDH release, TEER and histology analyses). These concentrations were relatively higher as compared to

other studies using organotypic tissue models; concentrations of 10 and 16% CS were used to test the effects of CS exposure in nasal and bronchial tissue models (Hoeng et al., 2013; Iskandar et al., 2013; Talikka et al., 2014). The lower sensitivity of the oral epithelia to CS exposure is likely due to their stratified and squamous structures, within which comprising more than 10 layers of flattened and terminally differentiated cells. These cells at the mucosal surface could shield the basal and suprabasal layers from exposure because the latter exert a proliferative characteristic and contain metabolically active keratinocytes (Figure 3).

Regardless of these higher concentrations of CS that were used in this study, our results indicated that signs of pronounced adaptive changes, tissue damage, or overt toxicity were not observed in these buccal and gingival organotypic tissue models (based on the outcomes of these classical cytotoxicity assays). This observation was also supported by the network-based systems biology approach; we detected only a weak impact of CS exposure on the Necroptosis network (Figure 6E and F). Further analysis of its subnetworks indicated some degrees of impact of CS on the FAS Activation, TNFR1 Activation and RIPK-ROS Mediated Execution subnetworks, suggesting that the network-based approach was relatively more sensitive to detect systems perturbation as compared to classical cytotoxic assays (e.g. LDH release or TEER assays).

Xenobiotic metabolism reflects the effects of CS exposure

Using various approaches, we found that CS exposure impacted xenobiotic metabolism in both buccal and gingival tissues. First, pathway annotations using DAVID indicated ''Metabolism of xenobiotics by P450s'' and ''Steroid hormone biosynthesis'' significantly enriched only in the *in vitro* datasets from the tissues exposed to the higher concentration of CS (Figure 4A and B). Regardless of the pathway names, both annotations were associated with genes encoding the phase I and phase II xenobiotic enzymes (Supplemental Table S2). This observation is also consistent with our comparative enrichment analysis, in which it resulted in significant annotation of ''Metabolism of xenobiotics by P450s.'' The common CS-related signature included upregulation of phase I enzymes *CYP1A1*, *CYP1B1*, *ALDH*, isoforms of *AKR1C* and phase II enzymes isoforms of *UGT* and *GPX2*, a pattern that may in the future also serve as a potential biomarker panel for translational studies to investigate the effects of CS exposure.

Second, using the network-based systems biology approach, we identified perturbations of biological network that indicated significant impact of CS on xenobiotic metabolism. Xenobiotic metabolism subnetwork, which is one of the subnetworks within the Stress network (Westra et al., 2011), was the primary subnetwork contributed to the overall score of exposure impact (Figure 6). Moreover, the impact of CS on the Stress network itself was the most consistent throughout the post-exposure time-points in both buccal and gingival tissues (Figure 5). In addition, impacts on the NFE2L2 Signaling subnetwork, which is a key mechanism of the phase II metabolism, also strongly contributed to the CS impact on the Stress network (Figure 6).

Finally, we also detected increased activity of CYP1A1/1B1, which belong to the phase I xenobiotic metabolizing enzymes and are known to be responsible for the metabolism of CS components. Both tissue types had low constitutive CYP1A1/CYP1B1 activities inferred by the observed activity in the air-exposed control. This is in agreement to what was observed previously in the EpiOral™ buccal tissue model by Walle et al. (2006). Other studies have also reported that buccal epithelial cells *in vitro* exhibit active metabolism of tobacco smoke constituents, such as nicotine-derived nitrosamine ketone [i.e. 4-(methylnitrosamino)-1-(3-pyridyl)-1-butanone] and benzo[a]pyrene (Autrup et al., 1985; Liu et al., 1993).

The increased activity of xenobiotic metabolism upon CS exposure is consistent with other publications. Xenobiotic metabolism machinery is responsible to handle toxicants, including CS components, which involves detoxification, transport and elimination (Iskandar et al., 2013). We have previously reported that examining the alterations in xenobiotic metabolism could be a sensitive approach to assess the impact of CS exposure; we reported that perturbation of xenobiotic metabolism could be utilized to compare the effect of CS *in vitro* with *in vivo* situation (Hoeng et al., 2013; Iskandar et al., 2013). Furthermore, Spivack et al. (2004) observed a strong correlation between smoking and the expression of genes encoding xenobiotic enzymes *CYP1B1* and *GSTP1* in exfoliated buccal epithelial cells obtained from oral brushings. Many studies have reported that oral tissues express a broad spectrum of xenobiotic-metabolizing enzymes, such as various CYPs, alcohol dehydrogenases, aldehyde dehydrogenases, aldo-keto reductases and various phase II enzymes (Hedberg et al., 2001; Liu et al., 1993; Spivack et al., 2004; Vondracek et al., 2001, 2002).

CS exposure elicits inflammatory responses

Inflammatory responses are known to be associated with smoking. In the current study, we detected many inflammatory mediators secreted into the culture media that indicated inflammatory responses in the tissues exposed to CS. Although the patterns of the secreted mediators were not similar between buccal and gingival tissue (Figure 8C), the protein abundance of both MMP-1 and VEGF was found to be consistently increased in both tissues following CS exposure. Increased MMP-1 in oral inflammation has been reported before in oral inflammatory models (i.e. lichen planus; Kim et al., 2006) and in bronchial tissue culture models exposed to CS (Mathis et al., 2013). Furthermore, increased VEGF protein abundance was also reported to be associated with oral inflammation, such as in gingival epithelium lining odontogenic cysts *in vivo* (Rubini et al., 2011). In addition, decreased levels of IP-10 were observed following the higher concentration of CS exposure in both the buccal and gingival tissues. This is consistent with the observation of Gemmell and colleagues, in which a decreasing number of IP-10-positive keratinocytes was found in the *in vivo* gingival epithelia samples that was inversely correlated with the severity of the inflammatory disease periodontitis (Gemmell et al., 2001). Furthermore, our group also detected increased VEGF and decreased

IP-10 secretion in organotypic tissue cultures of bronchial and nasal epithelium exposed to CS (Talikka et al., 2014). Therefore, increased secretion of VEGF and decreased secretion of IP-10 seems to be consistent in all four organotypic tissue models (i.e. nasal, bronchial, buccal and gingival) following exposure to CS. Nonetheless, the overall pattern of inflammatory markers that were secreted upon CS exposure among the buccal, gingival, nasal and bronchial tissue culture models seem to be not identical.

Moreover, the results showed that the changes of cytokine protein abundance (Figure 8C) that were measured at the 24 h post-exposure were not correlated with the mRNA expression measured at 0, 4 or 24 h (Figure 8D). There are various elements that may explain this discrepancy. First, the abundance of the proteins was measured in the basolateral medium of the tissues at 24 h following CS exposure, whereas the mRNA expression was generated from different tissue inserts, each of which was collected at the specific post-exposure time-points (i.e. they are not longitudinal data). Second, the measured protein abundance at the 24 h may reflect the accumulated cytokines in the medium, whereas the mRNA expression only reflects the transcript levels of the corresponding cytokines at the particular time-points when the tissues were harvested. Third, the increased cytokines abundance in response to CS exposure may in turn regulate their transcription in a different manner. Previous publications have reported that IL-4 and IFN-γ inhibit *MMP1* gene expression, whereas IL-1 and TNFα stimulate its transcription (Chakraborti et al., 2003; Vincenti et al., 1996).

In addition, using the network-based approach analysis, we found that the Pulmonary Inflammation network/subnetworks were impacted by CS in the tissue models (Figure 6). In the construction of biological network models, the Pulmonary Inflammation network (a.k.a. Pulmonary Inflammatory Process network (Westra et al., 2013)) contains many subnetworks related to various types of immune cells. Therefore, for this study, we selectively applied three selected subnetworks that are strictly associated with cellular responses of epithelial cells: Epithelial Proinflammatory Signaling, Epithelial Cell Barrier Defense and Tissue Damage subnetworks (Table 1). In addition, because Langerhans cells were included for the construction of the buccal tissue models, the three dendritic cell-specific subnetworks of the Pulmonary Inflammation network were included for the analysis of transcriptomics data from the buccal tissues: Dendritic Cell Activation, Dendritic Cell Migration to Tissue, Dendritic Cell Migration to Lymph Node (Table 1).

In contrast, pathways annotation of the *in vitro* dataset using DAVID did not support the occurrence of inflammatory responses in the *in vitro* tissues following CS exposure (Figure 4). The annotation of ''Arachidonic acid metabolism'' – which often indicate inflammatory processes – was applicable only from the comparative enrichment analysis with the *in vivo* dataset derived from buccal biopsies of smokers (Boyle et al., 2010; Figure 7E). This discrepancy may suggest that the DAVID analysis tool alone might not be sufficiently robust/sensitive to identify the entire biological processes affected by the exposure.

Applicability of organotypic tissues to *in vitro* exposure inhalation for toxicity testing

The application of tissues that are isolated from the upper respiratory tract is desirable because their collection is less invasive as compared to those of the lower respiratory tract. Studies have supported that buccal and gingival, as well as nasal tissues were suitable surrogates for bronchial tissues (Gower et al., 2011; Spira et al., 2007; Steiling et al., 2008). In regard to smoking, the oral tissues are more intensely and proportionally exposed to CS as compared to the nasal tissues. Oral mucosa is exposed to each puff of smoke that subsequently reaches the lung, whereas nasal mucosa is typically exposed to the exhaled lung-filtered smoke and occasionally to the inhaled side-stream smoke of smoldering cigarettes. Therefore, a smoke exposure to the oral tissue would be less variable as compared to the nasal tissue.

Studies have reported that reconstituted organotypic tissues of the oral cavity, such as 3D oral mucosal tissues (MatTek, SkinEthics), had differentiated characteristics similar to those of the *in vivo* tissues. Thus, they are considered to be relevant and suitable for studying the biology and pathology of the oral mucosa (e.g. inflammatory oral disease, gingivitis, candidiasis and oral cancer), as well as its innate immunity (Andrian et al., 2004; Ceder et al., 2007; Hansson et al., 2001; Klausner et al., 2007; Mostefaoui et al., 2002; Moyes et al., 2010; Walle et al., 2006; Wang et al., 2001). Our results further supported the before-mentioned publications, in which the impact of CS exposure including secretion of inflammatory markers could be assessed using the buccal and gingival organotypic tissue models. However, the buccal and gingival tissues that were used in the study were constructed from a single donor; therefore, whether similar impact could be reproduced when using different donors is unknown. This should be addressed in future studies, in which the impact of CS on 3D cultures of various tissue types obtained from different donors would be examined.

In addition, as surrogates of bronchial tissues, the nasal and oral tissues could be applied for the assessment of lung cancer risk. According to ''the field of injury'' hypothesis (Gower et al., 2011; Spira et al., 2007; Steiling et al., 2008), the cancer-related biomarkers appear to have a gradient effect from oral < nasal < bronchial epithelial samples concerning the strength of correlation with the primary (pre)neoplastic lesion in the lung. Whether this phenomenon can be reflected in *in vitro* organotypic culture models is unknown because ''the field of injury'' effect occurring *in vivo* may take decades to emerge. Future studies could address this question by conducting studies over an extended period of time – e.g. repeated exposure for several weeks to months. In contrast, such studies would be difficult to implement using monolayer cultures, suggesting another advantage of the organotypic culture models.

Although our studies and others supported that *in vitro* oral tissues reflected the effects of CS in the target tissue, translating the impact of *in vitro* exposures to the development of disease biomarkers remains challenging. In addition, smoking-related oral disease risks involve additional factors such as irritancy, infection, loss of protective mechanisms and genotoxicity. Therefore, our systems biology approach would

be superior to understand the complex nature of exposure and its impacts. Finally, to generate a more complete risk assessment, genotoxicity test, such as aneuploidy and chromosomal instability assays could be incorporated in future studies (Giaretti et al., 2012a,b; Pentenero et al., 2009).

Conclusion and outlook

We have demonstrated the usefulness of *in vitro* exposure to buccal and gingival organotypic epithelial tissue cultures for the impact assessment of CS. Furthermore, the applicability of multiple systems toxicology approaches and computational modeling for toxicity testing of CS exposure using the oral tissue models was reported in this current work. The most pronounced exposure effects were observed in xenobiotic metabolism. A weak inflammatory response was also observed, although the inflammatory responses appear to vary from those observed in bronchial or nasal epithelia exposed to CS. The comparative enrichment analysis generated from the gene expression profiles suggested similar biological pathways/mechanisms associated with smoke exposure between the *in vitro* and *in vivo* buccal samples.

Within our systems toxicology framework, we attempt to combine the results from *in vitro* models of oral (buccal and gingival), nasal and bronchial epithelium – the ''smoke street'' concept – when assuming that these respiratory tissues would complement rather than substitute one another. This concept, combined with our systems biology approach, aim to extrapolate a matrix of biomarkers for the assessment of CS effects, which eventually would enable a translation to disease risk. In such a framework, the oral, nasal and bronchial organotypic tissues would be useful tools to address the properties of reduced-risk products as compared with conventional reference cigarette smoke (3R4F), while also reducing the use of animals for inhalation studies.

Acknowledgements

The authors acknowledge the technical expertise of Emmanuel Guedj, Rémi Dulize, Dariusz Peric, Karine Baumer for the RNA sample processing and transcriptomics data generation. The authors also thank Céline Merg for the analysis of pro-inflammatory markers. We also thank Grégory Vuillaume for the statistical evaluation of LDH, TEER and CYP activity assays.

Declaration of interest

All authors are currently employed or formerly employed (MG) by Philip Morris International R&D. This study was funded by Philip Morris International R&D.

References

Ackermann M, Strimmer K. (2009). A general modular framework for gene set enrichment analysis. BMC Bioinformatics 10:47.

Andrian E, Grenier D, Rouabhia M. (2004). In vitro models of tissue penetration and destruction by Porphyromonas gingivalis. Infect Immun 72:4689–98.

Aufderheide M, Scheffler S, Mohle N, et al. (2011). Analytical in vitro approach for studying cyto- and genotoxic effects of particulate airborne material. Anal Bioanal Chem 401:3213–20.

Autrup H, Seremet T, Arenholt D, et al. (1985). Metabolism of benzo[a]pyrene by cultured rat and human buccal mucosa cells. Carcinogenesis 6:1761–5.

Balharry D, Sexton K, Berube KA. (2008). An in vitro approach to assess the toxicity of inhaled tobacco smoke components: nicotine, cadmium, formaldehyde and urethane. Toxicology 244:66–76.

Banerjee AG, Bhattacharyya I, Vishwanatha JK. (2005). Identification of genes and molecular pathways involved in the progression of premalignant oral epithelia. Mol Cancer Ther 4:865–75.

Bolstad BM, Irizarry RA, Astrand M, Speed TP. (2003). A comparison of normalization methods for high density oligonucleotide array data based on variance and bias. Bioinformatics 19:185–193.

Boyle JO, Gumus ZH, Kacker A, et al. (2010). Effects of cigarette smoke on the human oral mucosal transcriptome. Cancer Prev Res (Phila) 3: 266–78.

Ceder R, Merne M, Staab CA, et al. (2007). The application of normal, SV40 T-antigen-immortalised and tumour-derived oral keratinocytes, under serum-free conditions, to the study of the probability of cancer progression as a result of environmental exposure to chemicals. Altern Lab Anim 35:621–39.

Chakraborti S, Mandal M, Das S, et al. (2003). Regulation of matrix metalloproteinases: an overview. Mol Cell Biochem 253:269–85.

Chen YK, Hsue SS, Lin LM. (2005). Expression of p63 protein and mRNA in oral epithelial dysplasia. J Oral Pathol Med 34:232–9.

Chinnathambi S, Tomanek-Chalkley A, Ludwig N, et al. (2003). Recapitulation of oral mucosal tissues in long-term organotypic culture. Anat Rec A Discov Mol Cell Evol Biol 270:162–74.

Combes RD. (2004). The use of human cells in biomedical research and testing. Altern Lab Anim 32:43–9.

Dabija-Wolter G, Bakken V, Cimpan MR, et al. (2013). In vitro reconstruction of human junctional and sulcular epithelium. J Oral Pathol Med 42:396–404.

Dwivedi N, Chandra S, Kashyap B, et al. (2013). Suprabasal expression of Ki-67 as a marker for the severity of oral epithelial dysplasia and oral squamous cell carcinoma. Contemp Clin Dent 4:7–12.

Efron B, Tibshirani R. (2007). On testing the significance of sets of genes. Ann Appl Stat 1:107–29.

Gautier L, Cope L, Bolstad BM, Irizarry RA. (2004). Affy-analysis of Affymetrix GeneChip data at the probe level. Bioinformatics 20: 307–15.

Gebel S, Lichtner RB, Frushour B, et al. (2013). Construction of a computable network model for DNA damage, autophagy, cell death, and senescence. Bioinform Biol Insights 7:97–117.

Gemmell E, Carter CL, Seymour GJ. (2001). Chemokines in human periodontal disease tissues. Clin Exp Immunol 125:134–41.

Giaretti W, Maffei M, Pentenero M, et al. (2012a). Genomic aberrations in normal appearing mucosa fields distal from oral potentially malignant lesions. Cell Oncol (Dordr) 35:43–52.

Giaretti W, Pentenero M, Gandolfo S, Castagnola P. (2012b). Chromosomal instability, aneuploidy and routine high-resolution DNA content analysis in oral cancer risk evaluation. Future Oncol 8:1257–71.

Gonzalez-Suarez I, Sewer A, Walker P, et al. (2014). Systems biology approach for evaluating the biological impact of environmental toxicants in vitro. Chem Res Toxicol 27:367–76.

Gower AC, Steiling K, Brothers II JF, et al. (2011). Transcriptomic studies of the airway field of injury associated with smoking-related lung disease. Proc Am Thorac Soc 8:173–9.

Hansson A, Bloor BK, Haig Y, et al. (2001). Expression of keratins in normal, immortalized and malignant oral epithelia in organotypic culture. Oral Oncol 37:419–30.

Hatakeyama S, Yaegashi T, Takeda Y, Kunimatsu K. (2007). Localization of bromodeoxyuridine-incorporating, p63- and p75(NGFR)-expressing cells in the human gingival epithelium. J Oral Sci 49:287–91.

Hedberg JJ, Grafstrom RC, Vondracek M, et al. (2001). Micro-array chip analysis of carbonyl-metabolising enzymes in normal, immortalised and malignant human oral keratinocytes. Cell Mol Life Sci 58: 1719–26.

Hoeng J, Deehan R, Pratt D, et al. (2012). A network-based approach to quantifying the impact of biologically active substances. Drug Discov Today 17:413–18.

Hoeng J, Talikka M, Martin F, et al. (2013). Case study: the role of mechanistic network models in systems toxicology. Drug Discov Today 19:183–92.

Homann N, Karkkainen P, Koivisto T, et al. (1997). Effects of acetaldehyde on cell regeneration and differentiation of the upper gastrointestinal tract mucosa. J Natl Cancer Inst 89:1692–7.

Huang W, Sherman BT, Lempicki RA. (2009). Systematic and integrative analysis of large gene lists using DAVID bioinformatics resources. Nat Protoc 4:44–57.

International Organization for Standardization. (2010). ISO 3402: 1999 – Tobacco and tobacco products – Atmosphere for conditioning and testing, 4th ed. Geneva: ISO.

Iskandar AR, Martin F, Talikka M, et al. (2013). Systems approaches evaluating the perturbation of xenobiotic metabolism in response to cigarette smoke exposure in nasal and bronchial tissues. Biomed Res Int 2013:512086.

Jones KB, Klein OD. (2013). Oral epithelial stem cells in tissue maintenance and disease: the first steps in a long journey. In J Oral Sci 5:121–9.

Khan I, Agarwal P, Thangjam GS, et al. (2011). Role of TGF-beta and BMP7 in the pathogenesis of oral submucous fibrosis. Growth Factors 29:119–27.

Kim SG, Chae CH, Cho BO, et al. (2006). Apoptosis of oral epithelial cells in oral lichen planus caused by upregulation of BMP-4. J Oral Pathol Med 35:37–45.

Klausner M, Ayehunie S, Breyfogle BA, et al. (2007). Organotypic human oral tissue models for toxicological studies. Toxicol In Vitro 21:938–49.

Kupfer DM, White VL, Jenkins MC, Burian D. (2010). Examining smoking-induced differential gene expression changes in buccal mucosa. BMC Med Genomics 3:24.

Liu Y, Sundqvist K, Belinsky SA, et al. (1993). Metabolism and macromolecular interaction of the tobacco-specific carcinogen 4-(methylnitrosamino)-1-(3-pyridyl)-1-butanone in cultured explants and epithelial cells of human buccal mucosa. Carcinogenesis 14: 2383–8.

Marcelo CL, Peramo A, Ambati A, Feinberg SE. (2012). Characterization of a unique technique for culturing primary adult human epithelial progenitor/''stem cells''. BMC Dermatol 12:8.

Martin F, Thomson TM, Sewer A, et al. (2012). Assessment of network perturbation amplitudes by applying high-throughput data to causal biological networks. BMC Syst Biol 6:54.

Mathis C, Poussin C, Weisensee D, et al. (2013). Human bronchial epithelial cells exposed in vitro to cigarette smoke at the air-liquid interface resemble bronchial epithelium from human smokers. Am J Physiol Lung Cell Mol Physiol 304:L489–503.

Maunders H, Patwardhan SR, Phillips J, et al. (2007). Human bronchial epithelial cell transcriptome: gene expression changes following acute exposure to whole cigarette smoke in vitro. Am J Physiol Lung Cell Mol Physiol 292:L1248–56.

Mezentsev A, Amundson SA. (2011). Global gene expression responses to low- or high-dose radiation in a human three-dimensional tissue model. Radiat Res 175:677–88.

Mostefaoui Y, Claveau I, Ross G, Rouabhia M. (2002). Tissue structure, and IL-1beta, IL-8, and TNF-alpha secretions after contact by engineered human oral mucosa with dentifrices. J Clin Periodontol 29:1035–41.

Moyes DL, Runglall M, Murciano C, et al. (2010). A biphasic innate immune MAPK response discriminates between the yeast and hyphal forms of *Candida albicans* in epithelial cells. Cell Host Microbe 8: 225–35.

Noutomi Y, Oga A, Uchida K, et al. (2006). Comparative genomic hybridization reveals genetic progression of oral squamous cell carcinoma from dysplasia via two different tumourigenic pathways. J Pathol 210:67–74.

Office of the Surgeon General US. (2004). The Health Consequences of Smoking: A Report of the Surgeon General. Atlanta, GA: Centers for Disease Control and Prevention (US).

Paszkiewicz GM, Timm Jr EA, Mahoney MC, et al. (2008). Increased human buccal cell autofluorescence is a candidate biomarker of tobacco smoking. Cancer Epidemiol Biomarkers Prev 17:239–44.

Pentenero M, Giaretti W, Navone R, et al. (2009). DNA aneuploidy and dysplasia in oral potentially malignant disorders: association with cigarette smoking and site. Oral Oncol 45:887–90.

Port JL, Yamaguchi K, Du B, et al. (2004). Tobacco smoke induces CYP1B1 in the aerodigestive tract. Carcinogenesis 25:2275–81.

Proia NK, Paszkiewicz GM, Nasca MA, et al. (2006). Smoking and smokeless tobacco-associated human buccal cell mutations and their association with oral cancer – a review. Cancer Epidemiol Biomarkers Prev 15:1061–77.

R Development Core Team. (2010). R: a language and environment for statistical computing. Vienna, Austria: R Foundation for Statistical Computing.

R Development Core Team. (2012). R: a language and environment for statistical computing. With complete agglomeration and Euclidean distance metrics. Vienna, Austria: R Foundation for Statistical Computing.

Rowat JS, Squier CA. (1986). Rates of epithelial cell proliferation in the oral mucosa and skin of the tamarin monkey (*Saguinus fuscicollis*). J Dental Res 65:1326–31.

Rubini C, Artese L, Zizzi A, et al. (2011). Immunohistochemical expression of vascular endothelial growth factor (VEGF) in different types of odontogenic cysts. Clin Oral Investig 15:757–61.

Sasco AJ, Secretan MB, Straif K. (2004). Tobacco smoking and cancer: a brief review of recent epidemiological evidence. Lung Cancer 45: S3–9.

Schlage WK, Westra JW, Gebel S, et al. (2011). A computable cellular stress network model for non-diseased pulmonary and cardiovascular tissue. BMC Syst Biol 5:168.

Smyth GK. (2004). Linear models and empirical bayes methods for assessing differential expression in microarray experiments. Stat Appl Genet Mol Biol 3:Article 3.

Spira A, Beane JE, Shah V, et al. (2007). Airway epithelial gene expression in the diagnostic evaluation of smokers with suspect lung cancer. Nat Med 13:361–6.

Spivack SD, Hurteau GJ, Jain R, et al. (2004). Gene-environment interaction signatures by quantitative mRNA profiling in exfoliated buccal mucosal cells. Cancer Res 64:6805–13.

Sridhar S, Schembri F, Zeskind J, et al. (2008). Smoking-induced gene expression changes in the bronchial airway are reflected in nasal and buccal epithelium. BMC Genomics 9:259.

Steiling K, Ryan J, Brody JS, Spira A. (2008). The field of tissue injury in the lung and airway. Cancer Prev Res (Phila) 1:396–403.

Subramanian A, Tamayo P, Mootha VK, et al. (2005). Gene set enrichment analysis: a knowledge-based approach for interpreting genome-wide expression profiles. Proc Natl Acad Sci USA 102: 15545–50.

Talikka M, Kostadinova R, Xiang Y, et al. (2014). The response of human respiratory organotypic cultures to repeated cigarette smoke exposure. Int J Toxicol [submitted].

Terada M, Izumi K, Ohnuki H, et al. (2012). Construction and characterization of a tissue-engineered oral mucosa equivalent based on a chitosan-fish scale collagen composite. J Biomed Mater Res B Appl Biomater 100:1792–802.

Thomson TM, Sewer A, Martin F, et al. (2013). Quantitative assessment of biological impact using transcriptomic data and mechanistic network models. Toxicol Appl Pharmacol 273:863–78.

Toruner GA, Ulger C, Alkan M, et al. (2004). Association between gene expression profile and tumor invasion in oral squamous cell carcinoma. Cancer Genet Cytogenet 154:27–35.

Vincenti MP, White LA, Schroen DJ, et al. (1996). Regulating expression of the gene for matrix metalloproteinase-1 (collagenase): mechanisms that control enzyme activity, transcription, and mRNA stability. Crit Rev Eukaryot Gene Expr 6:391–411.

Vondracek M, Weaver DA, Sarang Z, et al. (2002). Transcript profiling of enzymes involved in detoxification of xenobiotics and reactive oxygen in human normal and simian virus 40 T antigen-immortalized oral keratinocytes. Int J Cancer 99:776–82.

Vondracek M, Xi Z, Larsson P, et al. (2001). Cytochrome P450 expression and related metabolism in human buccal mucosa. Carcinogenesis 22:481–8.

Walle T, Walle UK, Sedmera D, Klausner M. (2006). Benzo[A]pyrene-induced oral carcinogenesis and chemoprevention: studies in bio-engineered human tissue. Drug Metab Dispos 34:346–50.

Wang Y, Rotem E, Andriani F, Garlick JA. (2001). Smokeless tobacco extracts modulate keratinocyte and fibroblast growth in organotypic culture. J Dent Res 80:1862–6.

Warnakulasuriya S, Dietrich T, Bornstein MM, et al. (2010). Oral health risks of tobacco use and effects of cessation. Int Dent J 60:7–30.

Warnes GR, Bolker B, Bonebakker L, et al. (2012). gplots: Various R programming tools for plotting data (comprehensive R archive network). R package version 2.8.0. Available at: http://cran.r-project.org/web/packages/gplots/index.html webcite.

Watanabe S, Sato K, Okazaki Y, et al. (2009). Activation of PI3K-AKT pathway in oral epithelial dysplasia and early cancer of tongue. Bull Tokyo Dent Coll 50:125–33.

Westfall MD, Pietenpol JA. (2004). p63: molecular complexity in development and cancer. Carcinogenesis 25:857–64.

Westra JW, Schlage WK, Frushour BP, et al. (2011). Construction of a computable cell proliferation network focused on non-diseased lung cells. BMC Syst Biol 5:105.

Westra JW, Schlage WK, Hengstermann A, et al. (2013). A modular cell-type focused inflammatory process network model for non-diseased pulmonary tissue. Bioinform Biol Insights 7:167–92.

Winn DM. (2001). Tobacco use and oral disease. J Dent Educ 65: 306–12.

Wu C, Irizarry R. (2005). with contributions from Macdonald J, Genry J. gcrma: background adjustment using sequence information. 2.2.0 edition.

Yu CC, Woods AL, Levison DA. (1992). The assessment of cellular proliferation by immunohistochemistry: a review of currently available methods and their applications. Histochem J 24:121–31.

Zhang L, Rosin MP. (2001). Loss of heterozygosity: a potential tool in management of oral premalignant lesions? J Oral Pathol Med 30: 513–20.

Supplementary material available online

Supplemental Tables S1–S3 and Figures S1 and S2